

# Radiation-induced Luminescence Properties of Ce-doped SrAl<sub>2</sub>O<sub>4</sub> Crystal and Translucent Ceramic

Daisuke Nakauchi,\* Fumiya Nakamura, Takumi Kato,  
Noriaki Kawaguchi, and Takayuki Yanagida

Division of Materials Science, Nara Institute of Science and Technology,  
8916-5 Takayama, Ikoma, Nara 630-0192, Japan

(Received September 30, 2022; accepted January 11, 2023)

**Keywords:** scintillator, radioluminescence, photoluminescence, afterglow, pulse height

A comparative study on the radioluminescence properties of Ce-doped SrAl<sub>2</sub>O<sub>4</sub> single crystal and translucent ceramic was performed. The transmittance of the synthesized ceramic is 20–30% in the visible region. Both samples exhibit photo- and radioluminescence with a broad emission peaking at 380 nm. The decay curves are fitted by a single exponential decay function with decay time constants of 30–50 ns, consistent with the typical value of the emission for the 5d–4f transitions of Ce<sup>3+</sup>. From the pulse height spectra measured under <sup>241</sup>Am  $\gamma$ -ray (59.5 keV) irradiation, the scintillation light yields are 17000 ph/MeV for the single crystal and 6100 ph/MeV for the synthesized ceramic. The scintillation light yield and afterglow of the present samples show a negative correlation.

## 1. Introduction

Scintillators convert ionizing radiation into visible–UV photons, and they have been widely utilized to measure ionizing radiation in the fields of security,<sup>(1)</sup> medical imaging,<sup>(2,3)</sup> and resource exploration.<sup>(4,5)</sup> In general, required properties of scintillators include high scintillation output, short decay time, high energy resolution, and high effective atomic number; however, since no materials currently satisfy the requirements of all applications, R&D has been performed continuously on scintillators in various forms such as single crystals,<sup>(6–11)</sup> ceramics,<sup>(12–14)</sup> films,<sup>(15,16)</sup> glasses,<sup>(17–23)</sup> and liquids.<sup>(24–26)</sup>

Our research has focused on rare-earth-activated alkali-earth aluminates, which have been intensely studied in phosphor fields<sup>(27–29)</sup>; in particular, Eu,Dy-co-doped SrAl<sub>2</sub>O<sub>4</sub> is a well-known long-lifetime phosphorescent material.<sup>(30)</sup> We previously studied some alkali-earth aluminate compounds as scintillator candidates,<sup>(31–34)</sup> and we reported that SrAl<sub>2</sub>O<sub>4</sub> crystals doped with Eu exhibited a high scintillation light yield (*LY*).<sup>(32)</sup> Then, we focused on a translucent ceramic to improve the properties.<sup>(34)</sup> Because of their industrial advantages such as a low production cost, transparent ceramics have been mainly studied in the laser field.<sup>(35–37)</sup> In addition, for some radiation-induced phosphors, an improved scintillation *LY*<sup>(38)</sup> or storage

---

\*Corresponding author: e-mail: [nakauchi@ms.naist.jp](mailto:nakauchi@ms.naist.jp)  
<https://doi.org/10.18494/SAM4138>

luminescence has been reported.<sup>(39,40)</sup> In particular, spark plasma sintering (SPS) often enhances storage-luminescence properties because sintering in highly reductive conditions can generate defect centers. In this study, we investigated the radioluminescence and afterglow properties of both Ce-doped SrAl<sub>2</sub>O<sub>4</sub> single crystal and translucent ceramic. In recent years, radioluminescence and storage-luminescence properties have been found to be complementarily related in some materials<sup>(41)</sup> owing to energy conservation related to radiation-induced luminescence, and the systematic investigation of radiation-induced luminescence is important to comprehensively understand the luminescence phenomena induced by ionizing radiation.

## 2. Materials and Methods

A 1% Ce-doped SrAl<sub>2</sub>O<sub>4</sub> ceramic was synthesized using an SPS furnace (LabX-100, Sinter Land). A mixture of raw powders of CeO<sub>2</sub> (99.99%), SrCO<sub>3</sub> (99.99%), and Al<sub>2</sub>O<sub>3</sub> (99.99%) with a molar ratio of CeO<sub>2</sub>:SrCO<sub>3</sub>:Al<sub>2</sub>O<sub>3</sub> = 0.01:1:1 was sintered at 1450 °C for 10 min and then at 1600 °C for 20 min with a pressure of 70 MPa. A 1% Ce-doped SrAl<sub>2</sub>O<sub>4</sub> crystal was prepared by the floating zone (FZ) technique. A sintered precursor rod was loaded into an FZ furnace (FZD0192, Canon Machinery), and growth was conducted with a pulling speed of 5 mm/h and a rotation rate of 20 rpm. The photoluminescence (PL) spectra, decay time, and quantum yield (QY) were measured using Quantaaurus-QY and Quantaaurus-τ systems (C11347-01 and C11367, Hamamatsu Photonics). X-ray-induced radioluminescence (XRL) spectra, XRL decay time, afterglow, and pulse height were measured using a laboratory-made setup.<sup>(38,42)</sup>

## 3. Results and Discussion

The synthesized Ce:SrAl<sub>2</sub>O<sub>4</sub> crystal and ceramic samples are shown in Fig. 1. The crystal sample is colorless and transparent, while the ceramic sample is pale brown and translucent. Since only the ceramic was synthesized under reducing conditions, color centers such as oxygen defects are expected to be the cause of the pale brown appearance of the ceramic sample. Under UV irradiation (254 nm), blue luminescence due to Ce<sup>3+</sup> can be seen. The diffuse transmission spectra of the crystal and ceramic samples are shown Fig. 2. The crystal shows a transmittance of 70–80% in the visible range, while the ceramic shows a transmittance of 20–30%. In the spectra of the single crystal, strong absorption signals are observed at 260 and 320 nm owing to the 4f–5d<sub>2</sub> and 4f–5d<sub>1</sub> transitions of Ce<sup>3+</sup>, respectively.

The PL spectra of the crystal and ceramic samples are shown in Fig. 3. In both samples, excitation peaks appear at 260 and 325 nm, consistent with the absorption signals in Fig. 2. A broad emission at 380 nm is observed, whose origin is attributed to the 5d–4f transition of Ce<sup>3+</sup> from the past study of powder forms.<sup>(43–45)</sup> The QY values under excitation at 330 nm are 39% for the crystal and 10% for the ceramic. Figure 4 shows the PL decay time profiles monitored at 380 nm under excitation at 280 nm. From the calculation using least-squares fitting, the decay time constants is approximately 30 ns, which is a typical decay time constant for the 5d–4f transition of Ce<sup>3+</sup>.<sup>(46,47)</sup> No other components were detected.

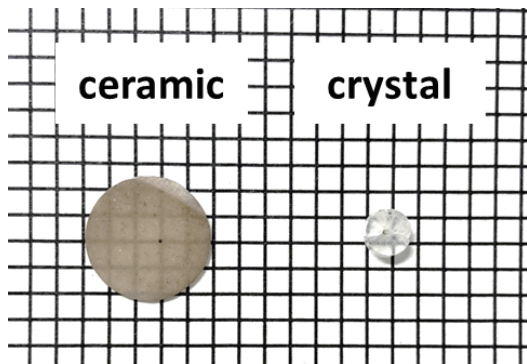


Fig. 1. (Color online) Photographs of  $\text{SrAl}_2\text{O}_4:\text{Ce}$  samples.

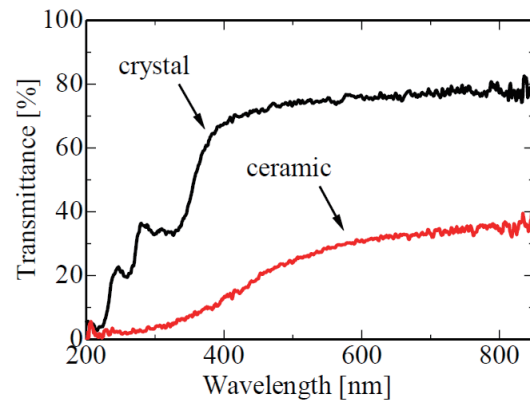


Fig. 2. (Color online) Diffuse transmission spectra of  $\text{SrAl}_2\text{O}_4:\text{Ce}$  samples.

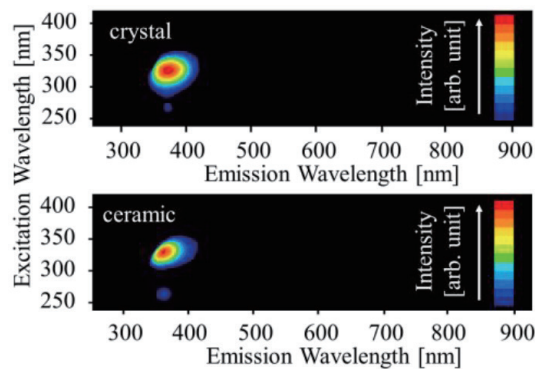


Fig. 3. (Color online) PL spectra of  $\text{SrAl}_2\text{O}_4:\text{Ce}$  samples.

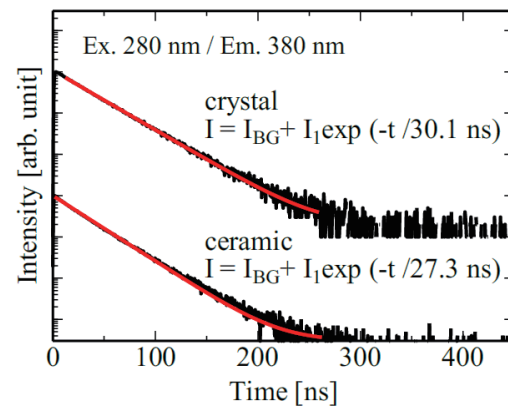


Fig. 4. (Color online) PL decay profiles of  $\text{SrAl}_2\text{O}_4:\text{Ce}$  samples.

The XRL spectra of  $\text{SrAl}_2\text{O}_4:\text{Ce}$  are shown in Fig. 5. A broad emission peak at 380 nm due to the  $5d-4f$  transition of  $\text{Ce}^{3+}$  is observed in both samples. The peak position in the ceramic sample slightly redshifts in comparison with that of the crystal sample because the crystal sample may have a lower dopant concentration than the ceramic sample because of segregation. The XRL decay time profiles of  $\text{SrAl}_2\text{O}_4:\text{Ce}$  are shown in Fig. 6. The decay curves are approximated by a single exponential decay function, and the decay time constants are 48.1 ns for the crystal sample and 45.2 ns for the ceramic sample. The obtained decay time constants are significantly larger than the PL decay owing to the different energy migration processes considered compared with PL. The PL decay reflects the direct excitation and relaxation at emission centers, while an additional transportation process from the host to emission centers occurs in scintillation.

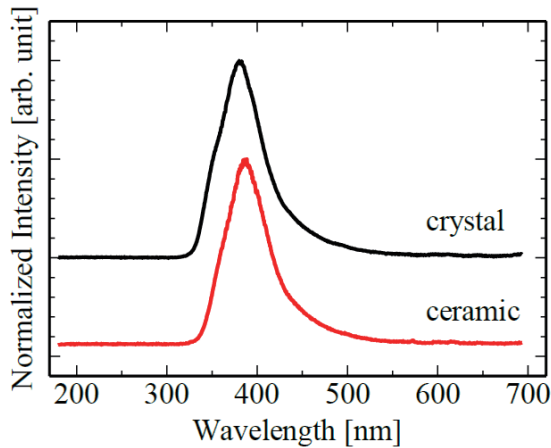


Fig. 5. (Color online) XRL spectra of  $\text{SrAl}_2\text{O}_4:\text{Ce}$ .

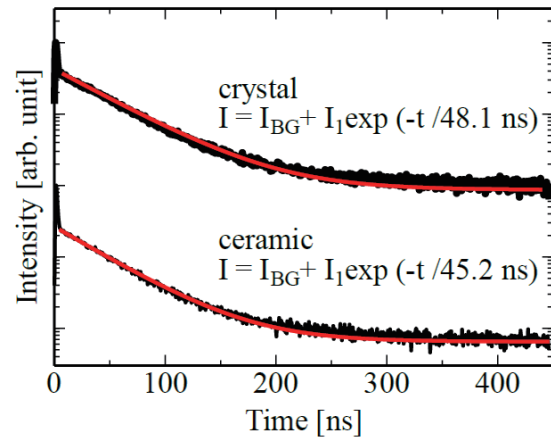


Fig. 6. (Color online) XRL decay profiles of  $\text{SrAl}_2\text{O}_4:\text{Ce}$ .

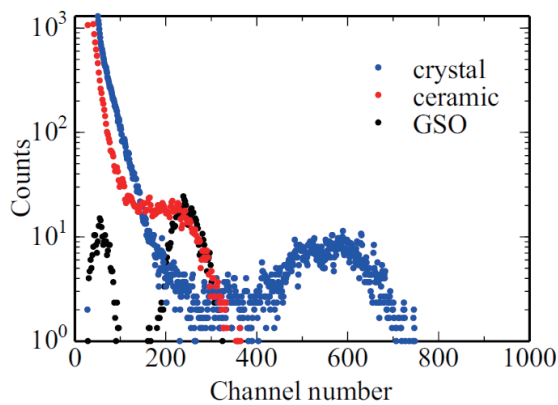


Fig. 7. (Color online) Measured pulse height spectra of  $\text{SrAl}_2\text{O}_4:\text{Ce}$  samples and reference GSO crystal.

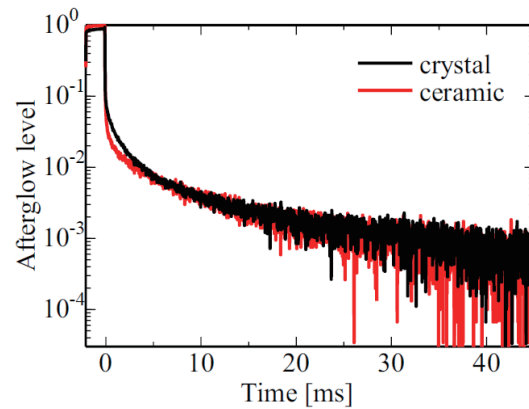


Fig. 8. (Color online) Afterglow curves of  $\text{SrAl}_2\text{O}_4:\text{Ce}$ .

The pulse height spectra under  $^{241}\text{Am}$   $\gamma$ -ray (59.5 keV) exposure are shown in Fig. 7. Here, the shaping time is 0.5  $\mu\text{s}$  for both the synthesized samples and a reference Ce-doped  $\text{Gd}_2\text{SiO}_5$  (GSO) crystal (OXIDE) with  $LY$  of 8000 ph/MeV. The crystal shows a clear photoabsorption peak at 600 ch, while the ceramic sample shows a shoulder-like peak at 213 ch. Taking into account the quantum efficiency of the photomultiplier tube (40% at 380 nm and 34% at 430 nm), the  $LY$  values of the crystal and ceramic samples are 17000 and 6100 ph/MeV, respectively.

The afterglow curves after X-ray irradiation for 2 ms are shown in Fig. 8. The afterglow level ( $AG$ ) was calculated using the equation  $AG = (I_2 - I_{BG}) / (I_1 - I_{BG})$ , where  $I_{BG}$ ,  $I_1$ , and  $I_2$  denote the signal intensities obtained before and during X-ray irradiation and at  $t = 20$  ms after X-ray cutoff, respectively. The  $AG$  values are 1460 ppm for the crystal and 1,900 ppm for the ceramic. The  $AG$  values of the present samples are much larger than those of practical X-ray scintillators such as  $\text{Bi}_4\text{Ge}_3\text{O}_{12}$  ( $\sim 10$  ppm).<sup>(42,48)</sup>

## 4. Conclusions

The PL, RL, and afterglow properties of the Ce-doped SrAl<sub>2</sub>O<sub>4</sub> crystal and ceramic samples were evaluated to investigate their dependence on the material form. The Ce-doped SrAl<sub>2</sub>O<sub>4</sub> crystal and ceramic samples show PL and RL signals peaking at 380 nm owing to the 5d–4f transition of Ce<sup>3+</sup>, and the decay time constants are almost the same as the typical values of Ce-doped phosphors. From the pulse height spectra, the *LY* values of the crystal and ceramic samples are 17000 and 6100 ph/MeV, respectively. The ceramic sample has a fourfold lower transmittance at the emission wavelength (380 nm) than the crystal sample, which would directly decrease *QY* fourfold. According to Robbins' theoretical formula,<sup>(49)</sup> *LY* is expressed as  $LY \propto S \times QY/E_{bg}$ , where *S* and *E<sub>bg</sub>* are the energy transport efficiency and bandgap energy, respectively. This formula suggests that *LY* is proportional to *QY*, and the results are consistent with the formula. Therefore, the low transmittance of the ceramic sample is considered to be related to the decrease in *LY*. In addition, *LY* and *AG* showed a negative correlation for both samples, which follows the energy conservation laws related to irradiation with ionizing radiation. Furthermore, the *AG* values of both samples are higher than those of practical scintillators. In our previous work,<sup>(33)</sup> the thermoluminescence properties of undoped and Ce-doped SrAl<sub>2</sub>O<sub>4</sub> were investigated. The undoped sample did not show a significant signal, while the Ce-doped sample showed a low-temperature peak that may have been related to *AG*. This is possibly due to charge compensation defects because of Ce doping, which would cause an increase in *AG* as well as a decrease in *LY*. On the basis of the energy conservation rule related to absorbed radiation energy, *LY* improves as *AG* is suppressed. One of the proposed means of suppressing *AG* is to reduce the number of defects by the charge compensation of Sr<sup>2+</sup> and Ce<sup>3+</sup> ions. To balance the charge, doping monovalent ions may suppress charge compensation defects.

## Acknowledgments

This work was supported by Grants-in-Aid for Scientific Research A (22H00309), B (21H03733, 21H03736, and 22H03872), and Exploratory Research (22K18997) from JSPS. A-STEP from JST, Foundation from Research Project of Research Center for Biomedical Engineering, Nippon Sheet Glass Foundation, Terumo Life Science Foundation, Iwatani Naoji Foundation, and Konica Minolta Science and Technology Foundation are also acknowledged.

## References

- 1 J. Glodo, Y. Wang, R. Shawgo, C. Brecher, R. H. Hawrami, J. Tower, and K. S. Shah: Phys. Procedia **90** (2017) 285. <https://doi.org/10.1016/j.phpro.2017.09.012>
- 2 S. Yamamoto, S. Okumura, N. Kato, and J. Y. Yeom: J. Instrum. **10** (2015) T09002. <https://doi.org/10.1088/1748-0221/10/09/T09002>
- 3 Y. Kurata, T. Usui, N. Shimura, S. Shimizu, and H. Ishibashi: Med. Imaging Technol. **27** (2009) 13. <https://doi.org/10.1149/mit.27.13>
- 4 C. L. Melcher: Nucl. Instrum. Methods Phys. Res. B **40–41** (1989) 1214. [https://doi.org/10.1016/0168-583X\(89\)90622-8](https://doi.org/10.1016/0168-583X(89)90622-8)
- 5 A. Baberdin, A. Dutova, A. Fedorov, M. Korzhik, V. Ligoun, O. Missevitch, V. Kazak, A. Vinokurov, and S. Zagumenov: IEEE Trans. Nucl. Sci. **55** (2008) 1170. <https://doi.org/10.1109/TNS.2008.919261>

- 6 M. Akatsuka, H. Kimura, D. Onoda, D. Shiratori, D. Nakauchi, T. Kato, N. Kawaguchi, and T. Yanagida: *Sens. Mater.* **33** (2021) 2243. <https://doi.org/10.18494/SAM.2021.3319>
- 7 D. Nakauchi, T. Kato, N. Kawaguchi, and T. Yanagida: *Sens. Mater.* **33** (2021) 2203. <https://doi.org/10.18494/SAM.2021.3323>
- 8 Y. Fujimoto, D. Nakauchi, T. Yanagida, M. Koshimizu, and K. Asai: *Sens. Mater.* **33** (2021) 2147. <https://doi.org/10.18494/SAM.2021.3321>
- 9 M. Koshimizu, N. Kawano, A. Kimura, S. Kurashima, M. Taguchi, Y. Fujimoto, and K. Asai: *Sens. Mater.* **33** (2021) 2137. <https://doi.org/10.18494/SAM.2021.3314>
- 10 K. Okazaki, D. Onoda, D. Nakauchi, N. Kawano, H. Fukushima, T. Kato, N. Kawaguchi, and T. Yanagida: *Sens. Mater.* **34** (2022) 575. <https://doi.org/10.18494/SAM3678>
- 11 D. Nakauchi, H. Fukushima, T. Kato, N. Kawaguchi, and T. Yanagida: *Sens. Mater.* **34** (2022) 611. <https://doi.org/10.18494/SAM3696>
- 12 R. Oh, S. Yanagisawa, H. Tanaka, T. Takata, G. Wakabayashi, M. Tanaka, N. Sugioka, Y. Koba, and K. Shinsho: *Sens. Mater.* **33** (2021) 2129. <https://doi.org/10.18494/SAM.2021.3328>
- 13 T. Kunikata, T. Kato, D. Shiratori, D. Nakauchi, N. Kawaguchi, and T. Yanagida: *Sens. Mater.* **34** (2022) 661. <https://doi.org/10.18494/SAM3683>
- 14 T. Kato, D. Nakauchi, N. Kawaguchi, and T. Yanagida: *Sens. Mater.* **34** (2022) 653. <https://doi.org/10.18494/SAM3682>
- 15 S. Matsumoto, A. Minamino, and A. Ito: *Sens. Mater.* **33** (2021) 2209. <https://doi.org/10.18494/SAM.2021.3325>
- 16 S. Matsumoto, T. Watanabe, and A. Ito: *Sens. Mater.* **34** (2022) 669. <https://doi.org/10.18494/SAM3698>
- 17 N. Kawaguchi, H. Masai, M. Akatsuka, D. Nakauchi, T. Kato, and T. Yanagida: *Sens. Mater.* **33** (2021) 2215. <https://doi.org/10.18494/SAM.2021.3410>
- 18 T. Yanagida, Y. Fujimoto, H. Masai, G. Okada, T. Kato, D. Nakauchi, and N. Kawaguchi: *Sens. Mater.* **33** (2021) 2179. <https://doi.org/10.18494/SAM.2021.3315>
- 19 N. Kawaguchi, D. Nakauchi, T. Kato, Y. Futami, and T. Yanagida: *Sens. Mater.* **34** (2022) 725. <https://doi.org/10.18494/SAM3705>
- 20 H. Fukushima, D. Shiratori, D. Nakauchi, T. Kato, N. Kawaguchi, and T. Yanagida: *Sens. Mater.* **34** (2022) 717. <https://doi.org/10.18494/SAM3691>
- 21 H. Kimura, T. Kato, D. Nakauchi, N. Kawaguchi, and T. Yanagida: *Sens. Mater.* **34** (2022) 691. <https://doi.org/10.18494/SAM3687>
- 22 G. Ito, H. Kimura, D. Shiratori, D. Nakauchi, T. Kato, N. Kawaguchi, and T. Yanagida: *Sens. Mater.* **34** (2022) 685. <https://doi.org/10.18494/SAM3681>
- 23 K. Ichiba, Y. Takebuchi, H. Kimura, D. Shiratori, T. Kato, D. Nakauchi, N. Kawaguchi, and T. Yanagida: *Sens. Mater.* **34** (2022) 677. <https://doi.org/10.18494/SAM3680>
- 24 M. Yeh, S. Hans, W. Beriguete, R. Rosero, L. Hu, R. L. Hahn, M. V. Diwan, D. E. Jaffe, S. H. Kettell, and L. Littenberg: *Nucl. Instrum. Methods Phys. Res. A* **660** (2011) 51. <https://doi.org/10.1016/j.nima.2011.08.040>
- 25 T. Doke, A. Hitachi, J. Kikuchi, K. Masuda, H. Okada, and E. Shibamura: *Jpn. J. Appl. Phys.* **41** (2002) 1538. <https://doi.org/10.1143/JJAP.41.1538>
- 26 A. Watanabe, A. Magi, M. Koshimizu, A. Sato, Y. Fujimoto, and K. Asai: *Sens. Mater.* **33** (2021) 2251. <https://doi.org/10.18494/SAM.2021.3411>
- 27 S. H. M. Poort, W. P. Blokpoel, and G. Blasse: *Chem. Mater.* **7** (1995) 1547. <https://doi.org/10.1021/cm00056a022>
- 28 T. Katsumata, T. Nabaie, K. Sasajima, and T. Matsuzawa: *J. Cryst. Growth* **183** (1998) 361. [https://doi.org/10.1016/0168-583X\(96\)00031-6](https://doi.org/10.1016/0168-583X(96)00031-6)
- 29 D. Ravichandran, S. T. Johnson, S. Erdei, R. Roy, and W. B. White: *Displays* **19** (1999) 197. [https://doi.org/10.1016/S0141-9382\(98\)00050-X](https://doi.org/10.1016/S0141-9382(98)00050-X)
- 30 T. Matsuzawa: *J. Electrochem. Soc.* **143** (1996) 2670. <https://doi.org/10.1149/1.1837067>
- 31 D. Nakauchi, G. Okada, M. Koshimizu, and T. Yanagida: *J. Rare Earths* **34** (2016) 757. [https://doi.org/10.1016/S1002-0721\(16\)60090-X](https://doi.org/10.1016/S1002-0721(16)60090-X)
- 32 D. Nakauchi, G. Okada, M. Koshimizu, and T. Yanagida: *J. Lumin.* **176** (2016) 342. <https://doi.org/10.1016/j.jlumin.2016.04.008>
- 33 D. Nakauchi, G. Okada, M. Koshimizu, and T. Yanagida: *Nucl. Instrum. Methods Phys. Res. A* **377** (2016) 89. <https://doi.org/10.1016/j.nimb.2016.04.017>
- 34 D. Nakauchi, F. Nakamura, G. Okada, H. Kimura, N. Kawaguchi, and T. Yanagida: *Radiat. Meas.* **126** (2019) 106127. <https://doi.org/10.1016/j.radmeas.2019.106127>
- 35 Y. Wu, J. Li, Y. Pan, J. Guo, B. Jiang, Y. Xu, and J. Xu: *J. Am. Ceram. Soc.* **90** (2007) 3334. <https://doi.org/10.1111/j.1551-2916.2007.01885.x>



- 36 R. Chaim, A. Shlayer, and C. Estournes: *J. Eur. Ceram. Soc.* **29** (2009) 91. <https://doi.org/10.1016/j.jeurceramsoc.2008.05.043>
- 37 H. Zhang, B. N. Kim, K. Morita, H. Yoshida, K. Hiraga, and Y. Sakka: *J. Am. Ceram. Soc.* **94** (2011) 3206. <https://doi.org/10.1111/j.1551-2916.2011.04789.x>
- 38 T. Yanagida, K. Kamada, Y. Fujimoto, H. Yagi, and T. Yanagitani: *Opt. Mater.* **35** (2013) 2480. <https://doi.org/10.1016/j.optmat.2013.07.002>
- 39 H. Kimura, F. Nakamura, T. Kato, D. Nakauchi, N. Kawano, G. Okada, N. Kawaguchi, and T. Yanagida: *J. Ceram. Soc. Jpn.* **126** (2018) 184. <https://doi.org/10.2109/jcersj2.17212>
- 40 N. Kawano, D. Nakauchi, K. Fukuda, G. Okada, N. Kawaguchi, and T. Yanagida: *Jpn. J. Appl. Phys.* **57** (2018) 102401. <https://doi.org/10.7567/JJAP.57.102401>
- 41 T. Yanagida: *Proc. Jpn. Acad. Ser. B* **94** (2018) 75. <https://doi.org/10.2183/pjab.94.007>
- 42 T. Yanagida, Y. Fujimoto, T. Ito, K. Uchiyama, and K. Mori: *Appl. Phys. Express* **7** (2014) 062401. <https://doi.org/10.7567/APEX.7.062401>
- 43 B. Y. Geng, J. Z. Ma, and F. M. Zhan: *J. Alloys Compd.* **473** (2009) 530. <https://doi.org/10.1016/j.jallcom.2008.06.014>
- 44 X. Xu, Y. Wang, X. Yu, Y. Li, and Y. Gong: *J. Am. Ceram. Soc.* **94** (2011) 160. <https://doi.org/10.1111/j.1551-2916.2010.04061.x>
- 45 R. Zheng, L. Xu, W. Qin, J. Chen, B. Dong, L. Zhang, and H. Song: *J. Mater. Sci.* **46** (2011) 7517. <https://doi.org/10.1007/s10853-011-5723-1>
- 46 L. Pidol, A. Kahn-Harari, B. Viana, E. Virey, B. Ferrand, P. Dorenbos, J. T. M. De Haas, and C. W. E. van Eijk: *IEEE Trans. Nucl. Sci.* **51** (2004) 1084. <https://doi.org/10.1109/TNS.2004.829542>
- 47 E. V. D. van Loef, P. Dorenbos, C. W. E. van Eijk, K. W. Krämer, and H. U. Güdel: *Nucl. Instrum. Methods Phys. Res. A* **486** (2002) 254. [https://doi.org/10.1016/S0168-9002\(02\)00712-X](https://doi.org/10.1016/S0168-9002(02)00712-X)
- 48 D. Nakauchi, T. Kato, N. Kawaguchi, and T. Yanagida: *Appl. Phys. Express* **13** (2020) 122001. <https://doi.org/10.35848/1882-0786/abc574>
- 49 D. J. Robbins: *J. Electrochem. Soc.* **127** (1980) 2694. <https://doi.org/10.1149/1.2129574>